The early angular momentum history of low mass stars: A surprising paradox

L. M. Rebull[1], S. C. Wolff[2], S. E. Strom[2], R. B. Makidon[3]

ABSTRACT

We examine the early angular momentum history of stars in young clusters via 197 photometric periods in fields flanking the Orion Nebula Cluster (ONC), 81 photometric periods in NGC 2264, and 202 measurements of $v \sin i$ in the ONC itself. We show that PMS stars, even those without observable disks, apparently do not conserve stellar angular momentum as they evolve down their convective tracks, but instead evolve at nearly constant angular velocity. This result is inconsistent with expectations that convective stars lacking disks should spin up as they contract, but paradoxically consistent with disk-locking models. We briefly explore possible resolutions to this paradox, including disk locking, birthline effects, stellar winds, and planetary companions.

Subject headings: stars: pre-main sequence — stars: rotation

1. Introduction

Observations over the past decade have established that pre-main sequence (PMS) stars accrete a substantial portion of their final mass via material transported through circumstellar disks. However, the prediction that accretion of high angular momentum disk material will cause the stars to spin up during the accretion phase (*e.g.* Durisen et al. 1989) is not borne out by observations: most PMS stars have rotational velocities (v) of no more than a few tens of km s^{-1}. By contrast, the typical breakup velocity at ~1 Myr is ~300 km s^{-1}.

Explanations of the observed slow rotation typically invoke angular momentum transfer either from the star to the surrounding accretion disk (*e.g.* Königl 1991), or to a stellar wind originating at the boundary between the disk and the stellar magnetosphere (*e.g.* Shu et al. 2000). Either mechanism requires that during the disk accretion phase, the angular velocity of the star be "locked" to a period set by the Keplerian angular velocity at the boundary between the stellar magnetosphere and the accretion disk. At the end of the accretion phase, PMS stars should be unlocked from their disks, and free to spin up as they contract toward the main sequence.

Considerable observational effort has been devoted to testing the prediction that rotation periods are locked to a narrow range during the accretion phase via comparison of the distribution of stellar periods or rotation rates for samples of stars surrounded by disks with those that lack disks. Early studies suggested that stars surrounded by disks tend to have significantly longer rotation periods than their diskless counterparts (*e.g.* Edwards et al. 1993, Choi & Herbst 1996); more recent results based on larger samples yield more ambiguous results. (*e.g.* Rebull 2001; Stassun et al. 1999).

[1]National Research Council Resident Research Associate, NASA/Jet Propulsion Laboratory, M/S 169-506, 4800 Oak Grove Drive, Pasadena, CA 91109 (luisa.rebull@jpl.nasa.gov)

[2]NOAO, 950 N. Cherry Ave, Tucson, AZ 87526

[3]STScI, 3700 San Martin Dr, Baltimore, MD 21218

for each cluster from the observed photometry and spectral types in the literature using exactly the same assumed photospheric colors and reddening law.

2.1. The ONC

The ONC has been studied recently by Rhode et al. (2001; RHM), who measured values of the projected rotational velocity ($v \sin i$) for 256 stars. In addition to providing a large and homogeneous data set, this study reached two conclusions that are relevant for the present discussion. First, RHM find no statistically significant difference between the $v \sin i$ distributions of PMS stars with known periods (P) and those without. Therefore, no statistical bias is introduced by the use of periods alone to study the rotational properties of young stars. Second, RHM calculate stellar radii ($R \sin i$) for those stars with known P and $v \sin i$. They find that, in the mean, these R values agree with the R values calculated from $L_{\rm bol}$ and $T_{\rm eff}$. For the sample taken as a whole, RHM also find evidence for PMS contraction as stars evolve down convective tracks at the 3-σ level. These results support the use of estimates of R derived from the apparent location of an individual star in the HRD as an independent variable that can be related directly to stellar age.

One advantage of using $v \sin i$ data is that line widths can be measured for every star that is observed (to the resolution limits of the study). Measurement of periods requires multiple observations, and certain P values may be missed because of the time intervals sampled. The lowest measurable $v \sin i$ is set by the spectral resolution. For the RHM data this is 11 km s^{-1}, which corresponds to P > 6 days for a typical PMS star. Stars rotating more slowly are included in the sample with this value as an upper limit.

The ONC is compact and young, with typical stellar ages of ~1–3 Myr (e.g. Hillenbrand 1997). It is also nearby; we have adopted a distance modulus of 8.36, or 470 pc, for Orion from Genzel et al. (1981). Observed V, $I_{\rm C}$, and K_s colors and spectral types for these stars were taken from Hillenbrand (1997). There are 202 stars for which both the photometry and measurements of $v \sin i$ are available; they appear in Figures 1–3. These figures show the observed and dereddened CMDs for the stars along with their positions in the $L_{\rm bol}$-$T_{\rm eff}$ plane.

About 60% of the stars in the $v \sin i$ sample have near-infrared ($I_{\rm C} - K_s$) excesses indicative of a circumstellar disk, e.g. a de-reddened $I_{\rm C} - K_s$ color exceeding expected photospheric values by 0.3 mag (cf. Hillenbrand 1997; Hillenbrand et al. 1998).

2.2. The Flanking Fields

The Orion Flanking Fields (FF) were defined and studied by Rebull et al. (2000) and Rebull (2001); we use $VI_{\rm C}K_s$ photometry, spectral types, and P from these papers, producing 197 stars which appear in Figures 1–3.

Measures of stellar rotation for this sample are provided by spot-modulated photometric periods (P). Spot modulation is only found in late-type stars, so unlike $v \sin i$ measurements which can be made of any type star, P observations are only obtainable for roughly types K and later. Period determinations have uncertainties δP <1%. The P measurements are sensitive to a broad range of periods, viz $P \sim 25 - 0.3$d, corresponding to rotational velocities $v \sim 3 - 300$ km s^{-1}, ranging from ~1–100% of the breakup velocity. We have limited our set of P data in Orion to the studies of the FF cited above because we wanted to be complete over the largest possible range of periods. Other Orion studies in the literature are complete over

amplitude of stellar variability, uncertainties in the reddening correction, errors in classification, uncertainties in the intrinsic photospheric colors, the effects of accretion, errors in the distance, and the presence of companions. All of these effects contribute to errors in $L_{\rm bol}$ and $T_{\rm eff}$ and hence to uncertainty in R. In the remainder of this section, we provide a thorough discussion of uncertainties involved in deriving $L_{\rm bol}$, $T_{\rm eff}$, and R from the observed colors and spectral types. Dominant errors are summarized in Table 1.

3.1. Errors in Brightness and Color

Photometric errors result from photon counting statistics, uncertainties in atmospheric extinction corrections, and uncertainties in transforming to a standard system. These errors are smallest for the brightest stars and largest for the faintest stars, but are typically ~0.03 mag in both $I_{\rm C}$ and $V - I_{\rm C}$.

Photometric variability on scales ranging from millimagnitudes to magnitudes is characteristic of young stars (e.g. Herbig 1954). The light curves of the P-selected samples (the FF and NGC 2264 stars) have typical amplitudes (mean-to-peak) of 0.03 mag in $I_{\rm C}$for all but the stars with spectral types M3 and later, which have somewhat larger amplitudes. The $v \sin i$ sample was specifically selected to include aperiodic as well as periodic variables. We do not have monitoring information on these specific stars, but the variations of similar aperiodic stars in the FF and NGC 2264 are strongly peaked near ~0.03 mag as well. We therefore take ~0.03 mag as the typical amplitude for all stars in our samples.

In our photometric studies of the FF and NGC 2264, we monitored in one filter, $I_{\rm C}$, only, and thus we do not have direct information on how $V - I_{\rm C}$ or V changes with these periodic modulations. Carpenter et al. (2001) monitored stars including those in 2 of the 4 FF in JHK_s. They find that most (57-77%) of their variable stars can be accounted for by cool spot models, e.g. low-amplitude, nearly colorless modulations. Based on this, we assume that the amplitude of variation we found at $I_{\rm C}$ also occurs in V, and that it does not affect $V - I_{\rm C}$ at significant levels.

If we assume that $V - I_{\rm C}$ is affected only by uncertainties resulting from photometric uncertainties, we derive uncertainties in luminosity $\delta \log L_{\rm bol}$ ~0.04; similarly $\delta \log T_{\rm eff} \sim 0.002$. Consequently, $\delta \log R = 1/2 \delta \log L_{\rm bol} + 2 \delta \log T_{\rm eff} \sim 0.02$. If we assume that $I_{\rm C}$ is affected by photometric uncertainties and by variations with an amplitude of 0.03 mag, we similarly derive $\delta \log L_{\rm bol} \sim 0.02$, and $\delta \log T_{\rm eff} \sim 0$ (because changing $I_{\rm C}$ alone does not change $T_{\rm eff}$), and thus $\delta \log R \sim 0.01$. These uncertainties increase with $V - I_{\rm C}$ primarily because the redder stars are also fainter.

3.2. Reddening corrections, photospheric colors, and spectral type uncertainties

We use spectral types to determine the intrinsic stellar colors and hence to derive (interstellar) reddening. The dominant error in this process is the uncertainty in spectral classification. Errors in typing have been estimated (Hillenbrand 1997, Rebull et al. 2000) at one subclass for the earlier types (F, G, K) and at half a subclass for the later types (M); it is more likely that the star will be incorrectly classified too early than too late because of the effects of veiling (e.g. Hillenbrand 1997).

Another potential source of error is uncertainty in the intrinsic photospheric colors. It is standard practice to adopt ZAMS colors as the best estimate for the true photospheric colors for these young, low-gravity stars. Our array of ZAMS colors includes measurements from Bessell (1991), Leggett (1992), and Leggett et al. (1998). This issue was discussed in detail by Rebull et al. (2000), so we only summarize some

3.4. Distance to and width of the clusters

Uncertainty in overall distance to the cluster results in a systematic shift of $L_{\rm bol}$ and R values. From the literature, the distance to Orion is 470±70 pc; that uncertainty of 70 pc translates directly to an uncertainty of 0.07 dex in log R. Similarly, NGC 2264 is at 760±30 pc, which translates to $\delta \log R$=0.03. Note, however, that an error in the average distance to a cluster simply introduces a systematic shift in $L_{\rm bol}$ or R for all the stars in the cluster. An error in distance does not therefore affect the *relative* values of R within the cluster but will affect comparisons of different clusters with each other.

The depths along the line of sight of the three groups of stars studied here are likely too small to affect the relative values of $L_{\rm bol}$ (and thus R) within a given cluster. The ONC is not much deeper than it is wide; at most generous, it is ±0.5 degree from the Trapezium stars, which is only about 1% of the distance to the cluster. The scatter in luminosity introduced by variations in the distance to individual stars is thus much smaller than other sources of error. As argued above, in the case of the FF, the presence of the molecular cloud and the evident association with and similarity to the young stars in the central ONC all suggest that the distance and depth of the cluster in these fields cannot be significantly different from the distance and depth of the central ONC. The cluster NGC 2264 also has a molecular cloud behind it and its depth along the line of sight is again a small fraction of the distance to the cluster.

3.5. Binaries

The presence of binaries could significantly affect the measured $I_{\rm C}$ and therefore the derived $L_{\rm bol}$. The worst-case scenario is two equal-mass binaries, where the measured $L_{\rm bol}$ is actually twice what it should be for a single star; in this case, it would create a 0.15 dex change in log R. However, the stars studied here are unlikely to have companions with luminosity ratios less than about 5/1. For the ONC sample, RHM obtained spectra for all of their stars and would have seen double lines either directly or in the cross-correlation peaks had the ratios of luminosities been smaller than 5/1; they found only 7 binaries in their full 256-star sample. For the Orion FF and NGC 2264, the period sample is also unlikely to be contaminated by unresolved binaries with similar luminosities. Analysis of such putative binaries would reveal *two* peaks in the power spectrum analysis of their light curves were the luminosity ratio of secondary to primary much smaller than 1/5. Therefore we estimate that the increase in log $L_{\rm bol}$ as a result of unrecognized binaries cannot exceed 0.10 for any of our samples.

3.6. Final error bars

The errors estimated above are summarized in Table 1 for three different mass ranges. If we now take the individual errors in $L_{\rm bol}$ and $T_{\rm eff}$ from each of the sources listed and add them in quadrature, we find that the net *typical* error in all sources considered for types M2 and earlier is $\delta \log L_{\rm bol} \sim 0.08$, $\delta \log T_{\rm eff} \sim 0.015$, and $\delta \log R \sim 0.05$. The *average* error in R for types M2 and earlier is $\delta \log R \sim 0.07$ (note that the average includes a small number of objects with unusually large errors). Only six stars with types M2 or earlier have errors in log R that are greater than 0.11. For types M3 and later, the average $\delta \log R \sim 0.087$, and the maximum error in log R is 0.19. For comparison, we also calculated a "worst-case scenario" in which all of the errors conspired to create the largest net errors possible. The errors in log R, at worst, were 0.1 dex.

The errors in P are negligible, and so the only way to invalidate this result is to hypothesize that the errors in R are much larger than we have estimated–so large, in fact, that we cannot use R to sort stars by age. If there were a wide mixture of ages at each R value, then the spin-up expected for conservation of angular momentum in diskless stars would be masked by observational scatter.

The study of ONC by RHM, however, rules out the possibility of such large errors in R. In their analysis, they show that the values of R derived from P and $v \sin i$ are consistent with the values of R derived from $L_{\rm bol}$ and $T_{\rm eff}$ and that the contraction in R with age predicted by the models is indeed observed. Moreover, the RHM data provide a second confirmation that PMS stars during their early lifetimes do indeed evolve at constant angular velocity, as we show in the next section.

4.2. The ONC

If stars evolve at constant P, as Figures 4 and 5 show, then v/R is constant. In other words, a solid prediction based on the observations of NGC 2264 and the FF is that older stars with smaller radii should be rotating more slowly than younger stars with larger radii. If, on the other hand, angular momentum (J) is conserved during evolution, then vR is constant. The typical change in R over the populated portion of the convective tracks is about a factor of 3 (cf. Figures 4 and 5). If we take a typical value of v to be about 35 km s^{-1} for the youngest stars (see results of RHM below), then if J is conserved, the oldest stars should be rotating at more than 100 km s^{-1}. If angular velocity is conserved, then the oldest stars should be rotating at about 12 km s^{-1}.

We can now ask which of these predictions best fits the RHM data for the ONC. Figure 6 shows that the stars observed in the ONC span the mass range $\sim$0.15–2.5 $M_\odot$. Note also that stars evolve down convective tracks at nearly constant $T_{\rm eff}$. In order to track the evolution of angular momentum, we have followed RHM and sorted the stars by $L_{\rm bol}$ and $T_{\rm eff}$ and hence approximately by age and mass. Each vertical column in the grid shown in Figure 6 spans a range of masses of about 30% around the mean mass. The convective tracks are not exactly vertical in this diagram, and so some stars of a given mass may move from one column to the next adjacent one as they evolve down their tracks. However, given that the mean $v \sin i$ ($<v \sin i>$) at a given luminosity shows no systematic trend and only very small variations with log $T_{\rm eff}$, the small change in average mass with decreasing luminosity will not significantly bias the results.

As discussed above, the errors in log $L_{\rm bol}$ and log $T_{\rm eff}$ are estimated to be 0.08 and 0.015 respectively. The width of the bins into which the stars were placed are 0.37 in log $L_{\rm bol}$ and 0.048 in log $T_{\rm eff}$. It is therefore unlikely that the errors in deriving log $L_{\rm bol}$ and log $T_{\rm eff}$ are large enough to move a star further than to a bin just adjacent to the true location. In most of the mass ranges studied, the stars span nearly 1.5 in log $L_{\rm bol}$, and so the errors in log $L_{\rm bol}$ are not large enough to mask systematic trends in $<v \sin i>$ as a function of $L_{\rm bol}$. Because (cf. Figure 7) there are no systematic trends in $v \sin i$ with $T_{\rm eff}$ at constant $L_{\rm bol}$, errors in $T_{\rm eff}$ are not large enough to introduce or mask any systematic trends.

Figure 7 shows this same rectangular grid, but now with lines of constant radius superposed. Comparing this figure with Figure 6 shows that the data for stars in a given mass range typically span a factor of $\sim$3 in radius. The average value of $v \sin i$ for the stars within each of the grid boxes is also shown. The data are summarized in Table 6, which gives $<v \sin i>$, its standard deviation, and the number of stars in each grid box.

Examination of Figure 7 shows that stars near the tops of the convective tracks have $v \sin i$ typically

Detection of such disks via H_2 or CO emission awaits more sensitive measurements than possible at present. A search for dust-free gaseous disks with SIRTF appears to be the most promising near-term approach.

5.2. Radius Changes Reflect Initial Conditions (Birthline Effects) Rather Than Evolution

Suppose that (1) stars in Orion and NGC 2264 were born in a single burst of star formation ~1 Myr ago; (2) the range in L (equivalently R) for the PMS stars in these clusters does not reflect evolution down convective tracks, but rather differences in mass accretion rate ($\dot{M}$) that force stars to evolve along different 'birthlines' and therefore to arrive at different initial luminosities along the convective tracks (Palla & Stahler 1992); and (3) PMS stars are locked to a particular P so long as they are surrounded by accretion disks. In this picture, the observed distribution of stars along a convective track for a given mass then reflects a range of $\dot{M}$: protostars with higher $\dot{M}$ have larger initial radii and lie higher in the color-magnitude diagram following the end of the accretion phase (see also Hartmann et al. 1997). The similarity of P at different R then follows from the assumption that stars are locked to their disks for much (nearly all) of their ~1 Myr accretion phase.

The main difficulty with this proposal lies with the additional requirement that stellar L cannot have decreased much since the stars were deposited on their convective tracks. If stars that formed through high $\dot{M}$ and were initially deposited high on their convective tracks had subsequently evolved downwards, we would expect to see a 'tail' of stars that have spun up to shorter P mixed in with the ensemble of objects that started their evolution at smaller R. We do not. The only way to resolve this contradiction and still maintain conservation of stellar J would be to identify a mechanism for halting or slowing evolution of stars deposited high on their convective tracks for a time comparable to at least ~3 Myr.

5.3. Angular Momentum Loss via Stellar Winds

Stellar winds loaded onto open magnetic field lines can exert a spindown torque on stars. However, this mechanism appears to be ineffective for PMS stars because, during this phase of evolution, the timescale for spindown exceeds the evolutionary timescale by a few orders of magnitude (*e.g.* MacGregor and Charbonneau 1994) – fully convective stars are assumed to rotate as solid bodies, and the wind must slow down the entire star.

Calculations (*e.g.* Kawaler 1988) show that the rate of change of J depends on the product of the mass loss rate and the square of the Alfven radius, but the Alfven radius varies inversely as some power of the mass loss rate, with the specific power depending on the configuration of the magnetic field. For a field geometry "intermediate" between a dipolar and a radial field, dJ/dt does not depend on mass loss rate at all (Bouvier et al. 1997). The only circumstance under which magnetic winds could play an important role in slowing the rotation of PMS stars would be if there were some way in which to decouple the outer layers of the star from the interior, *i.e.* if J were conserved locally, and the wind had to slow down only a thin outer layer of the star. Such decoupling is not expected for fully convective stars.

A further challenge to any wind-driven J loss mechanism is the additional requirement that significant J loss would have to cease on timescales of no more than a few Myr in order to account for the significant population of stars that ultimately arrive on the main sequence as the rapid rotators observed in young clusters such as αPersei (*e.g.* Stauffer et al. 1989); such stars require spinup from the PMS to the ZAMS.

Solar Systems program which enabled analysis of the NGC 2264 data. We thank Mark Adams for multiple comments and support during the early phases of the investigation of periodic stars and the McDonald Observatory for the award of guest investigator time on the 0.9m telescope. The research described in this paper was partially carried out at the Jet Propulsion Laboratory, California Institute of Technology, under a contract with the National Aeronautics and Space Administration.

REFERENCES

Barnes, S. A. 2001, ApJ, 561, 1095

Bessell, M. S. 1991, AJ, 101, 662

Bouvier, J., Forestini, M., & Allain, S. 1997, A&A, 326, 1023

Carpenter, J. M., Hillenbrand, L. A., & Skrutskie, M., F. 2001, AJ, 121, 3160

Choi, P., & Herbst, W. 1996, AJ, 111, 283

D'Antona, F., & Mazzitelli, I., 1994, ApJS, 90, 467

Durisen, R. H., Yang, S., Cassen, P., & Stahler, S. 1989, ApJ, 345, 959

Edwards, S., Strom, S. E., Hartigan, P., Strom, K. M., Hillenbrand, L. A., Herbst, W., Attridge, J., Meriill, K. M., Probst, R., & Gatley, I., 1993, AJ, 106, 372

Genzel, R., Reid, J. J., Moran, J. M., & Downes, D. 1981, ApJ, 244, 884

Hartigan, P., Strom, K., & Strom, S., 1994, ApJ, 427, 961

Hartmann, L. 2001, AJ, 121, 1030

Hartmann, L., Cassen, P., & Kenyon, S. J. 1997, ApJ, 475, 770

Herbig, G. 1954, ApJ, 119, 483

Hillenbrand, L. A. 1997, AJ, 113, 1733

Hillenbrand, L. A., et al. 1998, AJ, 116, 1816

Kawaler, S. D. 1988, ApJ, 333, 236

Kearns, K., & Herbst, W., 1997, AJ, 114, 1098

Kearns, K., & Herbst, W., 1998, AJ, 116, 261

Königl, A. 1991, ApJ, 370, 39

Leggett, S. K. 1992, ApJS, 82, 351

Leggett, S. K., Allard, F., Hauschildt, P. H. 1998, ApJ, 509, 836

MacGregor, K. B., & Charbonneau, P. 1994, in ASP Conf. Ser. 64, Cool Stars, Stellar Systems, and the Sun, Eighth Cambridge Workshop, ed. J.-P. Caillaut (San Francisco:ASP), 174

Table 1. Mean magnitude of empirically-derived errors

category	uncertainty	<K5	K5−M2	>M2
photometric	$\delta\log T_{\rm eff}$	0	0	0
in I +	$\delta\log L_{\rm bol}$	0.017	0.025	0.022
amplitude	$\delta\log R$	0.008	0.012	0.011
photometric	$\delta\log T_{\rm eff}$	0.004	0.002	0.002
in $V-I$	$\delta\log L_{\rm bol}$	0.052	0.044	0.039
	$\delta\log R$	0.024	0.024	0.022
spec type	$\delta\log T_{\rm eff}$	0.013	0.012	0.010
	$\delta\log L_{\rm bol}$	0.047	0.063	0.119
	$\delta\log R$	0.023	0.032	0.060
net mean	$\delta\log T_{\rm eff}$	0.014	0.012	0.010
	$\delta\log L_{\rm bol}$	0.072	0.081	0.127
	$\delta\log R$	0.064	0.065	0.084
typical	$\delta\log T_{\rm eff}$		0.01	
	$\delta\log L_{\rm bol}$		0.08	
	$\delta\log R$		0.05	

Table 2. Distribution of $v \sin i$ for the ONC stars.

log $T_{\rm eff}$[a]→	A (3.730-3.682)		B (3.682-3.634)		C (3.634-3.586)		D (3.586-3.538)		E (3.538-3.490)	
log $L/L_\odot$[a]↓	$<v \sin i>$	num[b]	$<v \sin i>$	num	$<v \sin i>$	num	$<v \sin i>$	num	$<v \sin i>$	num
1 (1.48 - 1.11)	33±13	3	41±10	5						
2 (1.11 - 0.74)	30±4	6	26±6	4	14	1				
3 (0.74 - 0.37)	26±5	7	15±4	4	34±12	7	35±9	5		
4 (0.37 - 0.00)	19±7	2	17±3	13	17±3	18	23±4	17	34±15	3
5 (0.00 - −0.37)	12	1			20±8	6	19±3	41	19±2	22
6 (−0.37 - −0.74)					18±7	3	16±4	18	20±3	44

[a]Subdivisions defined exactly as in RHM; subdivisions according to $T_{\rm eff}$ and L correspond to subdivisions by M for stars on convective tracks, and with age for stars of a given M. Column A from RHM spans a larger range of masses than the other columns, which span log $M/M_\odot$ ~0.1 dex when calculated via D'Antona & Mazzitelli (1994) or Siess et al. (2000).

[b]Number of stars in the bin.

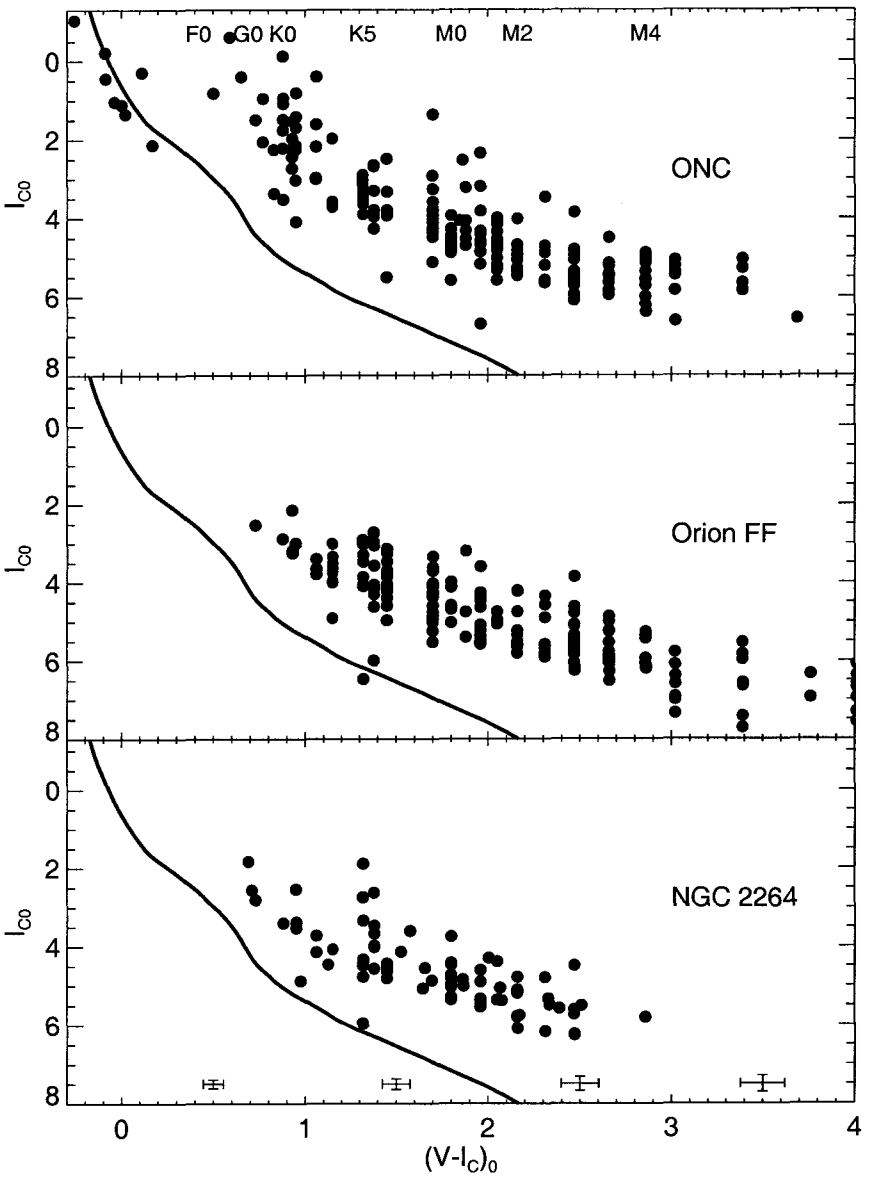

Fig. 2.— Dereddened CMD for each of the three samples considered in this paper: the Orion Nebula Cluster Flanking Fields, the Orion Nebula Cluster itself, and NGC 2264. I_C magnitudes have been corrected to absolute magnitudes for ease of comparison between the Orion samples and NGC 2264. $V - I_C$ values appear "quantized" because stars have been reddening-corrected to the intrinsic $V - I_C$ colors expected for their spectral types. ZAMS relation is heavy line, and $V - I_C$ colors of spectral types are indicated in top panel. In bottom panel, typical error bars are indicated for points with $V - I_C$ between 0–1, 1–2, 2–3, & 3–4; see text.

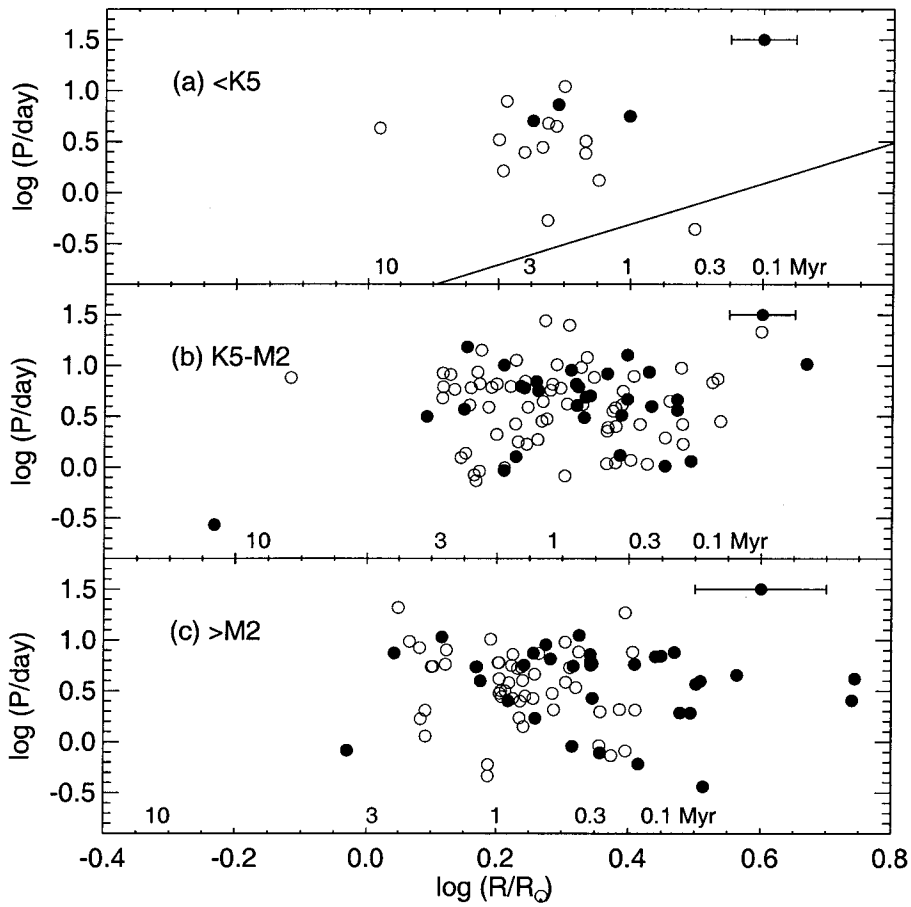

Fig. 4.— Period vs. radius for stars in the FF. (a) stars with types K5 and earlier; (b) stars with types K5-M2; (c) stars with types M3 and later. Open circles are stars without $I_C - K_s$ excesses (i.e. without disks) and solid circles are stars with excesses (i.e. with disks). Typical error bars for each type range are indicated. The line in panel (a) indicates the slope expected if stellar angular momentum is conserved.

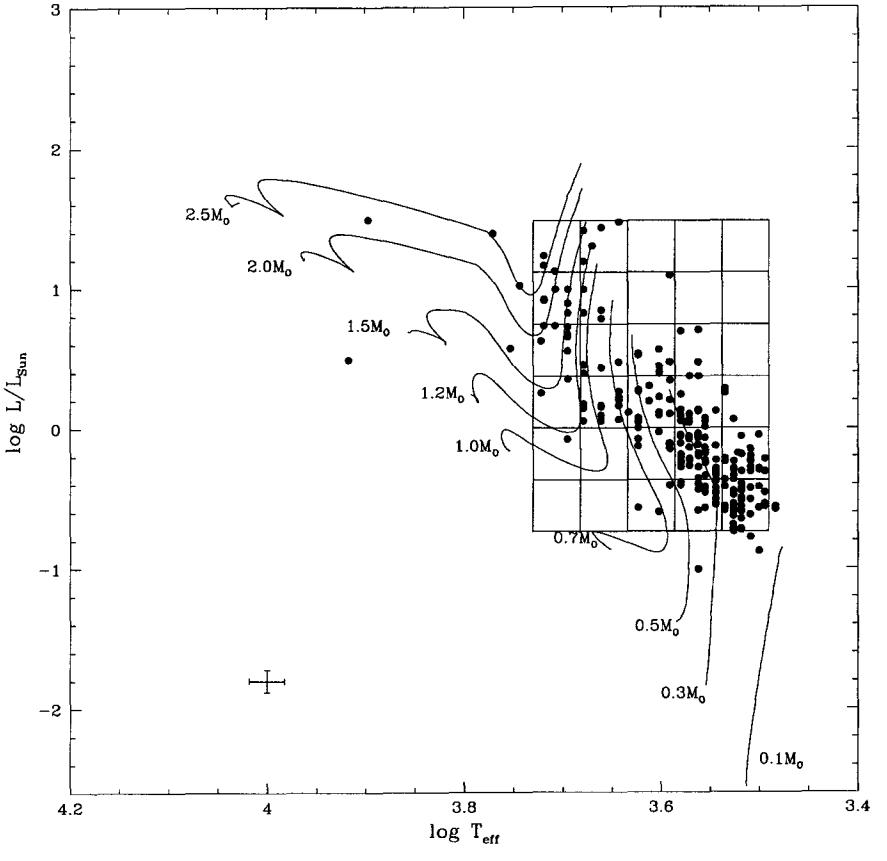

Fig. 6.— The HRD for the ONC stars. The evolutionary tracks are from D'Antona and Mazzitelli (1994). The grid shows the bins in the log $L_{\rm bol}$ and log $T_{\rm eff}$ plane into which we sorted the stars in order to look for trends in $<v \sin i>$ with decreasing luminosity and increasing age. The estimated error bars for log $L_{\rm bol}$ and log $T_{\rm eff}$ are given in the lower left corner of the plot.

Table 3. Trends in angular momentum ($\propto vR$) and angular velocity ($\propto v/R$) for the ONC.

$\log T_{\rm eff}$[a]→	A (3.730-3.682)		B (3.682-3.634)		C (3.634-3.586)	
$\log L/L_\odot$[a]↕	$< v\sin i > /R$[b]	$< v\sin i > \times R$[b]	$< v\sin i > /R$	$< v\sin i > \times R$	$< v\sin i > /R$	$< v\sin i > \times R$
1 (1.48 - 1.11)	6	191	6	296		
2 (1.11 - 0.74)	8	112	6	123	2	82
3 (0.74 - 0.37)	11	64	5	46	9	131
4 (0.37 - 0.00)	12	31	8	34	7	43
5 (0.00 - −0.37)	11	13			12	33
6 (−0.37 - −0.74)					17	19

[a]Subdivisions defined exactly as in RHM; subdivisions according to $T_{\rm eff}$ and L correspond to subdivisions by M for sta
A from RHM spans a larger range of masses than the other columns, which span $\log M/M_\odot \sim 0.1$ dex when calculated v

[b]$< v\sin i > /R$ would be constant if stellar J is conserved, and $< v\sin i > /R$ would be constant if ω conserved. No
within a factor of ∼2.